Mutagenesis, 2024, XX, 1–9
https://doi.org/10.1093/mutage/geae015
Advance access publication 6 June 2024
Original Manuscript

OXFORD

Original Manuscript

Fecal miRNA profiles in colorectal cancers with mucinous morphology

Alessio Naccarati[1,2,*], Mihnea P. Dragomir[3,4,5], Sonia Tarallo[1,2], Amedeo Gagliardi[1,2], Virginia Alberini[1,2,6], Tomas Buchler[7], Vaclav Liska[8,9,10], Gaetano Gallo[11,12], Veronika Vymetalkova[10], Ludmila Vodickova[8,10,13], Pavel Vodicka[8,10,13], Barbara Pardini[1,2], Giulio Ferrero[1,6]

[1]Genetic and Molecular Epidemiology Unit, Italian Institute for Genomic Medicine (IIGM), c/o IRCCS Candiolo, Candiolo 10060, Turin, Italy
[2]Candiolo Cancer Institute, FPO IRCCS, Candiolo 10060, Turin, Italy
[3]Institute of Pathology, Charité – Universitätsmedizin Berlin, Corporate Member of Freie Universität Berlin, Humboldt-Universität zu Berlin, Berlin 10117, Germany
[4]German Cancer Consortium (DKTK), Partner Site Berlin, and German Cancer Research Center (DKFZ), Heidelberg 69120, Germany
[5]Berlin Institute of Health at Charit´e - Universit¨atsmedizin Berlin, Charit´eplatz 1, 10117 Berlin, Germany
[6]Department of Clinical and Biological Sciences, University of Torino, Turin 10100, Italy
[7]Department of Oncology, Second Faculty of Medicine, Charles University and Motol University Hospital, Prague 150 06, Czech Republic
[8]Biomedical Centre, Faculty of Medicine in Pilsen, Charles University, Pilsen 32300, Czech Republic
[9]Department of Surgery, University Hospital and Faculty of Medicine in Pilsen, Charles University, Pilsen 32300, Czech Republic
[10]Department of Molecular Biology of Cancer, Institute of Experimental Medicine of the Czech Academy of Sciences, Prague 14220, Czech Republic
[11]Department of Surgery, "La Sapienza" University of Rome, Rome 00161, Italy
[12]Department of Colorectal Surgery, Clinica S. Rita, Vercelli 13100, Italy
[13]Institute of Biology and Medical Genetics, 1st Medical Faculty, Charles University, Prague 12800, Czech Republic

[*]Corresponding author. Genetic and Molecular Epidemiology Unit, Italian Institute for Genomic Medicine (IIGM), c/o IRCCS Candiolo, SP 142, Km 3.95, 10060 Candiolo, Torino, Italy. E-mail: alessio.naccarati@iigm.it

Abstract

The diagnostic performance of molecular markers in surrogate tissues like stool may be affected by colorectal cancer (CRC) morphological heterogeneity. The mucinous histotype represents a subgroup of CRC with a peculiar molecular program and unfavorable disease progression. However, the percentage of mucinous morphology necessary to define this subtype is still a matter of debate. In this study, we investigated whether stool miRNA profiles of CRC patients differ in patients with mucinous histopathological subtypes compared to non-mucinous cancers. In this respect, we also explored how the stool miRNA signature reported in our previous multicentric study behaves in this histotype. Small-RNA sequencing was performed in fecal and tissue samples of an Italian cohort ($n = 172$), including 27 CRC with mucinous morphology (mucinous cancers with ≥ 50% mucinous morphology and those with mucinous component ≥ 5% but < 50%), 58 non-mucinous CRC, and 87 colonoscopy-negative controls. Results were compared with fecal miRNA profiles of a cohort from the Czech Republic ($n = 98$). Most of the differentially expressed (DE) stool miRNAs ($n = 324$) were in common between CRC with mucinous morphology and non-mucinous histopathological subtypes in comparison with healthy controls. Interestingly, the altered levels of 25 fecal miRNAs previously identified distinguishing CRC cases from controls in both cohorts were also confirmed after stratification for mucinous morphology. Forty-nine miRNAs were DE exclusively in CRC with mucinous morphology and 61 in non-mucinous CRC. Mucinous cancers and those with mucinous component showed fairly similar profiles that were comparable in the Czech cohort. Among the stool DE miRNAs observed in CRC with mucinous morphology, 20 were also altered in the comparison between tumor and adjacent mucosa tissue. This study highlights miRNAs specifically altered in CRC with mucinous morphology. Nevertheless, the performance of our stool miRNA signature in accurately distinguishing CRC cases from controls was not significantly affected by this histological subtype. This aspect further supports the use of stool miRNAs for noninvasive diagnosis and screening strategies.

Keywords: stool miRNA signatures; colorectal cancer; mucinous morphology; tumor heterogeneity

Introduction

Colorectal cancer (CRC) classified as mucinous, is a distinct histological subtype of colorectal epithelial tumors with a frequency of 10–15% in sporadic cases. Except for tumor not otherwise specified, this is the most common histotype of CRC. The World Health Organization (WHO) defines mucinous CRC (mCRC) as invasive colon and rectum epithelial tumors characterized by extracellular mucinous components

Received 19 February 2024; accepted 5 June 2024
© The Author(s) 2024. Published by Oxford University Press on behalf of the UK Environmental Mutagen Society. All rights reserved. For commercial re-use, please contact reprints@oup.com for reprints and translation rights for reprints. All other permissions can be obtained through our RightsLink service via the Permissions link on the article page on our site—for further information please contact journals.permissions@oup.com.

Downloaded from https://academic.oup.com/mutage/advance-article/doi/10.1093/mutage/geae015/7689086 by Sapienza Università di Roma user on 30 June 2024

comprising at least 50% of the tumor area [1–3]. In addition, the WHO recommends for cases with < 50% mucinous morphology to use the term CRC with mucinous component (CRCmc). The designation of a tumor as mCRC or CRCmc is often dependent on the individual pathologist's assessment and level of experience. mCRC is graded based on the level of epithelial maturation and gland formation [3]. Nevertheless, grade assignment is largely subjective [4].

Among the unique clinical and histopathological characteristics of mCRC, there is a different response to therapies and a different prognosis when compared to non-mucinous CRC (nmCRC). CRC with mucinous morphology are more common in the proximal colon, are larger, have a higher T-stage, a higher proportion of positive lymph nodes, poorer tumor differentiation, and a higher proportion of peritoneal implants compared to nmCRC [5]. The etiology of this tumor histotype is not well understood; however, they are more frequently associated with microsatellite instability (MSI) and *BRAF*-mutated CRC pathways [6]. The clinical significance of mucinous morphology of CRC is underscored by two aspects: (i) shorter overall survival as highlighted by several studies [7,8] and (ii) poor response to chemotherapy and radiotherapy [9]. The debate concerning the prognostic implications of CRC with mucinous morphology is still open and is considered as an unfavorable subtype of the disease. Nevertheless, in the past few years, epidemiological and clinical studies have shed new light on the management of patients with this tumor histotype [4].

Evidence supports the expression of microRNAs (miRNAs), pivotal post-transcriptional regulator of gene expression [10], as biomarkers of specific CRC subtypes, including those from Consensus Molecular Subtype (CMS) [11], or from stratification based on specific mutational profiles [12]. Despite some authors previously described miRNAs specifically expressed in CRC with a mucinous morphology [13], little is known about the overall miRNome profile of this histotype. Recently, our group demonstrated that specific fecal miRNA profiles can accurately distinguish CRC and advanced adenoma patient samples from those of healthy control subjects [14]. The integration of fecal and tissue miRNA profiles can reveal novel molecular players involved in the definition of the mCRC and CRCmc phenotypes. In addition, such an approach could further reveal if our diagnostic signature is impacted by the tumor morphological characteristics and further test the robustness of our tool.

The present study investigated stool miRNA profiles in subjects diagnosed with mCRC or CRCmc with the aims to compare them with those from nmCRC. We also compared our previously identified miRNA signature from multiple CRC cohorts and performed an integrative analysis with miRNA profiles in CRC tissue samples.

Materials and methods

Study cohorts

Italian Study Cohort (IT-cohort)

The cohort includes 230 subjects recruited in a hospital-based study in Vercelli, Italy. Based on colonoscopy results, individuals were stratified in CRC patients ($n = 120$) and colonoscopy-negative controls ($n = 110$). Stool specimens were collected from 172 individuals (85 CRC and 87 controls) while primary tumor and matched adjacent mucosa tissue were collected for 100 CRC patients.

Czech Study Cohort (CZ-cohort)

Stool specimens as well as clinical and demographic data were collected from 98 Czech individuals recruited in two hospitals in Prague and one in Plzen, Czech Republic. Based on colonoscopy results, participants were divided into 61 CRC patients and 37 colonoscopy-negative individuals.

For both cohorts, colonoscopy was performed (i) because of the recommendation of the family doctor for various reasons (age of the patient, complaints in the gut, etc.) or (ii) because the patient had a positive screening result (i.e. there was blood in the stool at the time of the test, and therefore the individual was invited to have a colonoscopy to further investigate the reason for blood in stool).

A full description of the cohorts and the biospecimens collection is reported in [14,15].

The local ethics committees of Azienda Ospedaliera SS. Antonio e Biagio e C. Arrigo of Alessandria (Italy, protocol no. Colorectal miRNA CEC2014) and the Institute of Experimental Medicine of Prague (Czech Republic) approved the study. All patients gave written informed consent following the Declaration of Helsinki before participating in the study.

Pathology review and quantification of the mucinous histopathological subtype

All tumors of both IT- and CZ- cohorts were diagnosed by pathologists at the local hospital where samples were collected. Moreover, for this study, a pathologist experienced in gastrointestinal pathology (M.P.D.) additionally reviewed the histopathologic diagnosis of all specimens by analyzing resection samples. Briefly, one H&E-stained whole slide from each patient was analyzed using an Olympus BX46 microscope (Olympus Europe). The pathologist reviewed the diagnosis of CRC and quantified the mucinous component of each tumor in 5% increments. The mucinous subtype was quantified only for the invasive component of CRC, and the mucinous morphology of adjacent precursor lesions was not considered. Tumors with ≥ 50% mucinous morphology were defined as mCRC, while tumors with < 50% mucinous morphology were defined as CRCmc. All other samples were considered as nmCRC (**Fig. 1A**). Digital histologic images were obtained using the PANNORAMIC 1000 digital slide scanner (3DHISTECH).

Sample collection and nucleic acids extraction

All participants provided naturally evacuated fecal samples after being previously instructed to self-collect the specimen at home. Stool samples were collected in nucleic acid collection and transport tubes with RNA stabilizing solution (Norgen Biotek Corp). 200 µl stool aliquots were stored at −80°C until RNA extraction that was performed using the Stool Total RNA Purification Kit (Norgen Biotek Corp) as described in [16].

Primary tumor and adjacent mucosa (at least 20 cm distant) tissues from CRC subjects were collected during surgical resection and immediately transferred in cryogenic vials with RNAlater™ Solution (Invitrogen) and stored at −80°C until use. RNA from tissues was isolated using QIAzol (QIAGEN) after tissue homogenization performed

Downloaded from https://academic.oup.com/mutage/advance-article/doi/10.1093/mutage/geae015/7689086 by Sapienza Università di Roma user on 30 June 2024

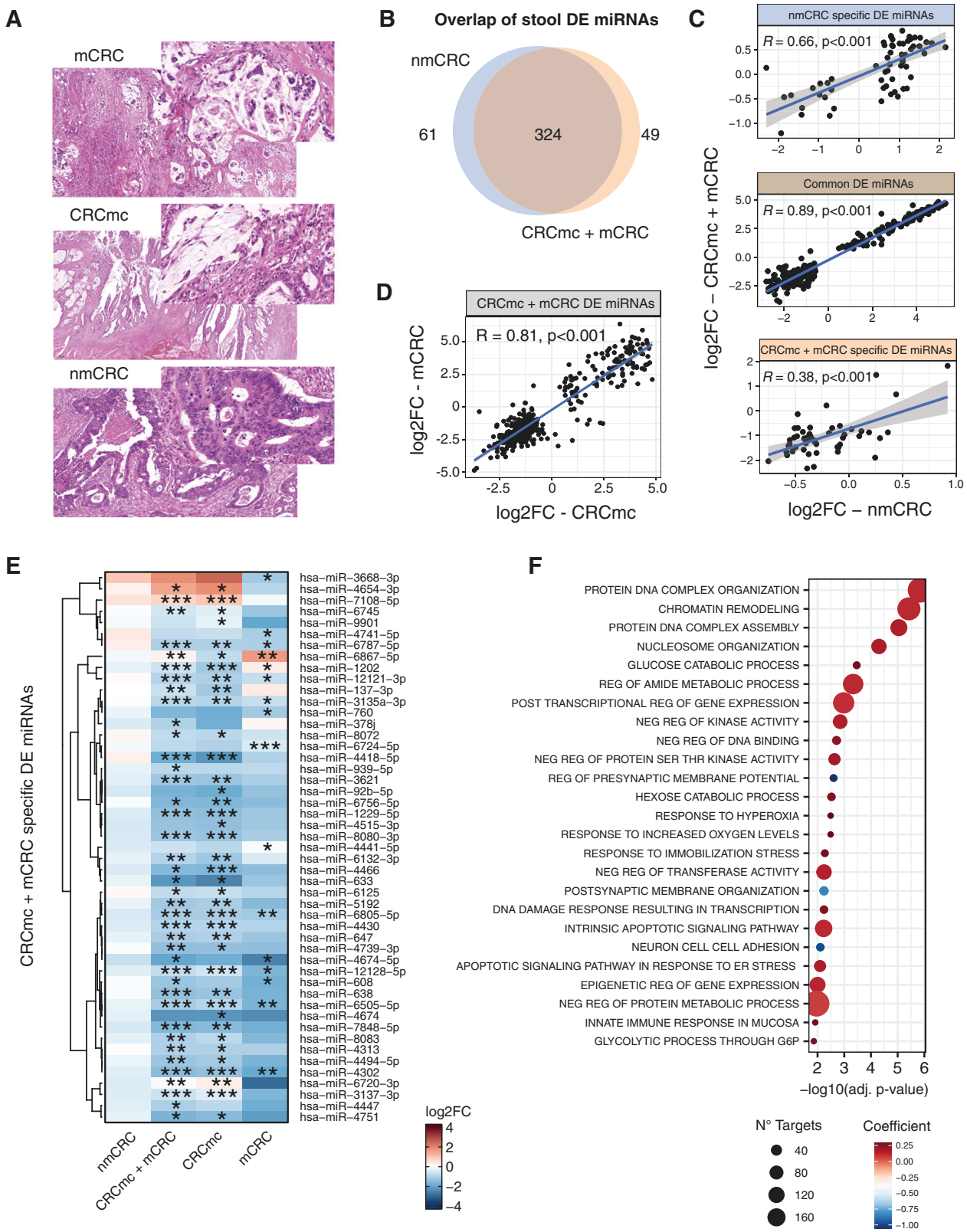

Figure 1. (A) Representative H&E images showing mucinous tumors (mCRC, up), tumors with mucinous component < 50% (CRCmc, middle), and non-mucinous (nmCRC, down); **(B)** Venn diagram of the overlap between stool differentially expressed (DE) miRNAs identified in nmCRC or in CRCmc and CRCm considered together. **(C)** Scatter plots of the log2FC of stool DE miRNA levels computed between nmCRC (x-axis) and CRCmc + mCRC (y-axis) with respect to healthy controls. The sets were defined based on the overlap reported in panel B. Spearman correlation coefficients are reported. **(D)** Scatter plot of the log2FC of stool DE miRNA levels computed between CRCmc (x-axis) and mCRC (y-axis) with respect to healthy controls. Data of all DE miRNAs obtained in the analysis of CRCmc and mCRC are reported. **(E)** Heat map of the log2FC of the 49 miRNAs specifically observed as DE in CRCmc and mCRC with respect to healthy controls. Adjusted *P*-value from DESeq2 analysis. *adj. $P < .05$; **adj. $P < .01$; ***adj. $P < .001$. **(F)** Dot plot of the significant Gene Ontology Biological Processes enriched in the 49 DE miRNA targets. Dot size is proportional to the number of target genes, while the color code represents the coefficient predicting whether the pathway is activated (red) or repressed (blue) based on DE miRNA expression changes.

Downloaded from https://academic.oup.com/mutage/advance-article/doi/10.1093/mutage/geae015/7689086 by Sapienza Università di Roma user on 30 June 2024

with ULTRA-TURRAX ® Homogenizer, followed by phenol/chloroform extraction according to the manufacturer's standard protocol.

DNA extraction from tissues was performed with Maxwell® RSC Tissue DNA Kit (Promega), with a preliminary homogenization step in a homogenization solution (Promega) (full description in [15]). DNA was quantified with Qubit™ 4 fluorometer using Qubit™ dsDNA High Sensitivity Assay Kit (Invitrogen).

Small RNA sequencing

Small RNA sequencing (sRNA-Seq) libraries were prepared from stool and tissue RNA using the NEBNext Multiplex Small RNA Library Prep for Illumina (New England Biolabs, Inc) kit as described in [17]. Briefly, 250 ng of stool/tissue RNA were converted into barcoded complementary DNA (cDNA) libraries. Each library was prepared with a unique indexed primer. Multiplex adapter ligations, RT primer hybridization, RT reaction, and PCR amplification were performed according to the manufacturer's protocol. After PCR amplification, the cDNA constructs were purified with the QIAQuick PCR Purification Kit (Qiagen), following the modifications suggested by the NEBNext Multiplex Small RNA Library Prep for Illumina protocol. Final libraries were loaded on the Bioanalyzer 2100 (Agilent Technologies) using the DNA High Sensitivity Kit (Agilent Technologies) according to the manufacturer's protocol. Libraries were pooled together (in 24-plex or 30-plex) and further purified with a gel size selection. A final Bioanalyzer 2100 run with the High Sensitivity DNA Kit (Agilent Technologies) allowed us to assess DNA library quality regarding size, purity, and concentration. The obtained libraries were subjected to the Illumina sequencing pipeline on Illumina HiSeq4000 and NextSeq500 sequencers (Illumina Inc) (75 cycles, single-end sequencing) as previously described in [17].

TruSight™ oncology 500 high-throughput

Mutational and MSI status of 106 CRC patients of the IT-cohort were assessed using the hybrid capture TruSight™ Oncology 500 High Throughput (TSO500-HT) kit (Illumina). DNA libraries were prepared following the Illumina® TruSight™ Oncology 500 Reference Guide. Details are reported in [15].

Computational and statistical analyses

sRNA-Seq data analyses were performed as described by [14] considering a curated miRNA reference based on miRBase v22.1. Differential expression analyses were performed using DESeq2 v1.22.2. A miRNA was considered as differentially expressed (DE) if associated with a median >15 of normalized reads count and with an adjusted *P*-value (adj. *P*) < .05. Functional enrichment analysis was performed with RBiomirGS v0.2.12 considering the validated miRNA-target interactions from miRTarBase 7.0 and miRecords.

Data produced by the TSO500-HT were analyzed with the Illumina TSO500 Local App (v 2.2) pipeline. Briefly, for each subject, files reporting information on quality controls, genetic variants, and tumor mutational burden were created. An in-house Python script was created to aggregate these files.

Results

Characteristics of the study cohort

Seven out of the 120 CRC patients of the IT-cohort showed a mucinous component greater than the WHO threshold of 50% and were classified as mCRC, while 29 tumors were characterized by a mucinous component between 5% and 50%. This latter group was hereafter defined as CRCmc (**Table 1**). The remaining 84 patients were categorized as nmCRC, being characterized by a tumor with no or less than 5% mucinous component. Analysis of the patient covariates showed that CRCmc patients were significantly older (73 ± 11 vs. 69 ± 10 years old; $P < .05$) and characterized by a lower BMI (24.4 ± 3.9 vs. 26.6 ± 5.3; $P < .05$) than nmCRC (**Table 1**). As expected, patients with mCRC were associated with a worst prognosis ($P < .05$). A higher proportion of invasive tumor (AJCC stage 3 and 4) characterized the CRCmc considered alone or together with mCRC ($P < .05$), while no significant differences in tumor localization were observed (**Table 1**). Mutational profiles based on target DNA sequencing showed a higher proportion of *BRAF*-mutated tumors among CRCmc and mCRC (considered together) compared to non-mucinous lesions ($P < .05$), while *APC* mutations were significantly more prevalent in nmCRC compared to CRCmc ($P < .05$). In addition, the proportion of MSI-high patients was higher in CRCmc compared to nmCRC ($P < .05$) (**Table 1**).

Fecal miRNA profiles of CRC with mucinous or non-mucinous morphology

Fecal sRNA-Seq data were available for 85 patients and were explored to identify candidate fecal miRNA profiles characterizing CRCmc or mCRC. From nmCRC to mCRC a slightly but not significant decrease in the number of detected fecal miRNAs was observed with a median of 397, 375, and 321 miRNAs detected in nmCRC, CRCmc, and mCRC, respectively. Overall, the number of detected miRNAs in all CRC patient subgroups was significantly lower ($P < .05$) than in healthy subjects (median = 511) (**Supplementary Table 1A**).

An age- and sex-adjusted differential expression analysis was performed between the fecal miRNA levels of nmCRC, CRCmc, and mCRC with respect to those of 87 colonoscopy-negative control subjects. In total, 385 miRNAs were significantly DE (median levels > 15 normalized reads and adj. $P < .05$) in stool from CRC patients compared to controls (**Fig. 1B** and **Supplementary Table 1B**). Among them, 324 (84.2%) were in common between nmCRC and CRCmc + mCRC (**Fig. 1B**). In addition, 49 fecal DE miRNAs were identified only in CRCmc or mCRC (individually or together) but not in nmCRC (**Fig. 1B**). Globally, the changes in fecal miRNAs were coherent between nmCRC and those with a mucinous morphology (CRCmc + mCRC) ($\rho = 0.73$, $P < .001$), particularly, as expected, for the common DE miRNAs ($\rho = 0.89$, $P < .001$) (**Fig. 1C**). A significant correlation was also observed by comparing the log2FC computed for the analysis of the two mucinous groups ($\rho = 0.81$, $P < 0.001$) (**Fig. 1D**). Indeed, among the 49 DE miRNAs, 41 (83.7%) were characterized by lower levels in both CRCmc and mCRC patient samples compared to those from healthy controls (**Fig. 1E** and **Supplementary Table 1B**). Conversely, seven DE miRNAs (miR-3668-3p, miR-4654-3p, miR-7108-5p, miR-6867-5p, miR-1202, miR-137-3p, miR-378j) were associated with an opposite log2FC between CRCmc and mCRC profiles. For 20 out of 49 DE miRNAs, lower fecal levels were observed by comparing the samples from CRCmc and mCRC with respect to those of nmCRC patients (**Supplementary Table 1B**).

Functional enrichment analysis

The analysis of the targets of the 49 fecal DE miRNAs evidenced 5,569 validated miRNA-target interactions involving 2,258 genes (**Supplementary Table 1C–D**). The gene targeted

Downloaded from https://academic.oup.com/mutage/advance-article/doi/10.1093/mutage/geae015/7689086 by Sapienza Università di Roma user on 30 June 2024

Table 1. Characteristics of the study population.

Characteristic	Class[a]			*P*-value[b]		
	nmCRC *N* = 84	CRCmc *N* = 29	mCRC *N* = 7	nmCRC vs. CRCmc + mCRC	nmCRC vs. CRCmc	nmCRC vs. mCRC
Age	69 (10)	73 (11)	71 (9)	.052	.037	.5
Sex				.8	>.9	.7
Female	37 (44%)	13 (45%)	2 (29%)			
Male	47 (56%)	16 (55%)	5 (71%)			
BMI	26.6 (5.3)	24.4 (3.9)	25.6 (3.9)	.036	.025	.7
Smoking				.3	.4	.4
Former	11 (14%)	6 (22%)	2 (33%)			
Never	40 (52%)	10 (37%)	3 (50%)			
Smoker	26 (34%)	11 (41%)	1 (17%)			
Unknown	7	2	1			
OS status				.10	.3	.041
Alive	66 (81%)	20 (71%)	3 (43%)			
Deceased	16 (19%)	8 (29%)	4 (57%)			
Unknown	1	1	0			
AJCC CRC Stage				.023	.019	.5
0	2 (3%)	0 (0%)	0 (0%)			
I	15 (20%)	9 (32%)	2 (29%)			
II	30 (39%)	4 (14%)	1 (14%)			
III	23 (30%)	15 (54%)	3 (43%)			
IV	6 (8%)	0 (0%)	1 (14%)			
Unknown	8	1	0			
Localization				.2	.2	.8
Proximal	28 (31%)	15 (52%)	3 (43%)			
Distal	25 (27%)	7 (24%)	1 (14%)			
Rectum	33 (39%)	7 (24%)	3 (43%)			
BRAF				.033	.095	.080
Mutated	4 (5%)	4 (17%)	2 (29%)			
WT	71 (95%)	20 (83%)	5 (71%)			
Unknown	9	5	0			
APC				.087	.010	.4
Mutated	48 (64%)	8 (33%)	6 (86%)			
WT	27 (36%)	16 (67%)	1 (14%)			
Unknown	9	5	0			
KRAS				.5	.8	.4
Mutated	19 (25%)	7 (29%)	3 (43%)			
WT	56 (75%)	17 (71%)	4 (57%)			
Unknown	9	5	0			
MSI				.077	.037	.4
High	4 (5%)	5 (21%)	1 (14%)			
Stable	70 (95%)	19 (79%)	6 (86%)			
Unknown	10	5	0			

[a]Mean (SD); *n* (%);
[b]Wilcoxon rank sum test; Fisher's exact test. nmCRC: non-mucinous tumors; CRCmc: tumors with mucinous component < 50%; mCRC: mucinous tumors.

by the highest number of DE miRNAs ($n = 8$) was *NACC1* followed by *SPRY4*, *NFIC*, and *DDA1* (each targeted by seven DE miRNAs) (Supplementary Table 1C–D). Conversely, the interactions supported by the highest number of independent studies were those between *DDX39B* and miR-4447, miR-608, miR-6756-5p (48 supporting studies), followed by miR-4430-*ABCF1* (14 studies) and miR-6805-5p-*ATG2A* (11 studies) interactions (Supplementary Table 1D). Functional enrichment analysis of these targets showed an enrichment of terms related to chromatin organization (e.g. *PROTEIN_DNA_COMPLEX_ORGANIZATION*, *CHROMATIN_REMODELING*, and *NUCLEOSOME_ORGANIZATION*), glucose metabolism (e.g. *HEXOSE_CATABOLIC_PROCESS*, *GLUCOSE_CATABOLIC_PROCESS*, and *REGULATION_OF_AMIDE_METABOLIC_PROCESS*), and stress response

Downloaded from https://academic.oup.com/mutage/advance-article/doi/10.1093/mutage/geae015/7689086 by Sapienza Università di Roma user on 30 June 2024

(e.g. *RESPONSE_TO_HYPEROXIA* and *RESPONSE_TO_IMMOBILIZATION_STRESS*) (Fig. 1F and Supplementary Table 1E).

Comparison with an independent cohort and with a previously identified set of CRC fecal miRNA biomarkers

The analysis of sRNA-Seq data of samples from an independent cohort of Czech CRC patients and controls (CZ-cohort), showed a decrease of the fecal DE miRNAs to 25 out of the 49 reported for the IT-cohort albeit the difference was statistically significant ($P < .05$) only for three miRNAs (miR-4751, miR-4447, and miR-4654-3p) (Supplementary Table 1B).

The set of fecal DE miRNAs identified in this study was compared with the 25 DE miRNAs characterizing CRC patients previously identified by us [14]. Among these 25 DE miRNAs, 19 were significantly differentially expressed in both nmCRC, CRCmc, and mCRC patients, while three (miR-149-3p, miR-4492, and miR-6131) remained DE only in nmCRC patients (Fig. 2 and Supplementary Table 1B). As for the whole DE miRNA set, also for these 25 miRNAs, the log2FCs computed between controls and the different CRC patient groups were significantly coherent (ρ: 0.94, $P < .001$). Similar coherence was observed also comparing the log2FCs computed for the CZ-cohort (ρ: 0.87, $P < .001$).

sRNA-Seq in tissue samples

miRNA levels were measured by sRNA-Seq also in tissue pairs from CRC patients of the IT-cohort, detecting a median of 670 miRNAs in each sample, with no significant differences between the average number of miRNAs detected in CRC and adjacent tissue data. In total, 491 DE miRNAs were identified between tumor and paired adjacent colonic mucosa (Supplementary Table 1B). Among them, 291 (59.27%) were commonly DE in both CRC with a mucinous morphology and in nmCRC. On the other hand, 158 miRNAs were DE only in the tissue of nmCRC patients, while 33 in the tissue of CRCmc or mCRC considered alone or together (median reads > 15 and adj. $P < .05$).

Considering the 373 DE miRNAs identified in fecal samples of mCRC + CRCmc patients, the analysis of their expression changes in tissue showed a slightly negative correlation with the changes observed in stool (ρ = −0.17, $P < .01$) (Fig. 3A). Among these miRNAs, 111 were differentially expressed also in the comparison of tissue samples (Supplementary Table 1B). Specifically, 69 tissue miRNAs were commonly DE in the

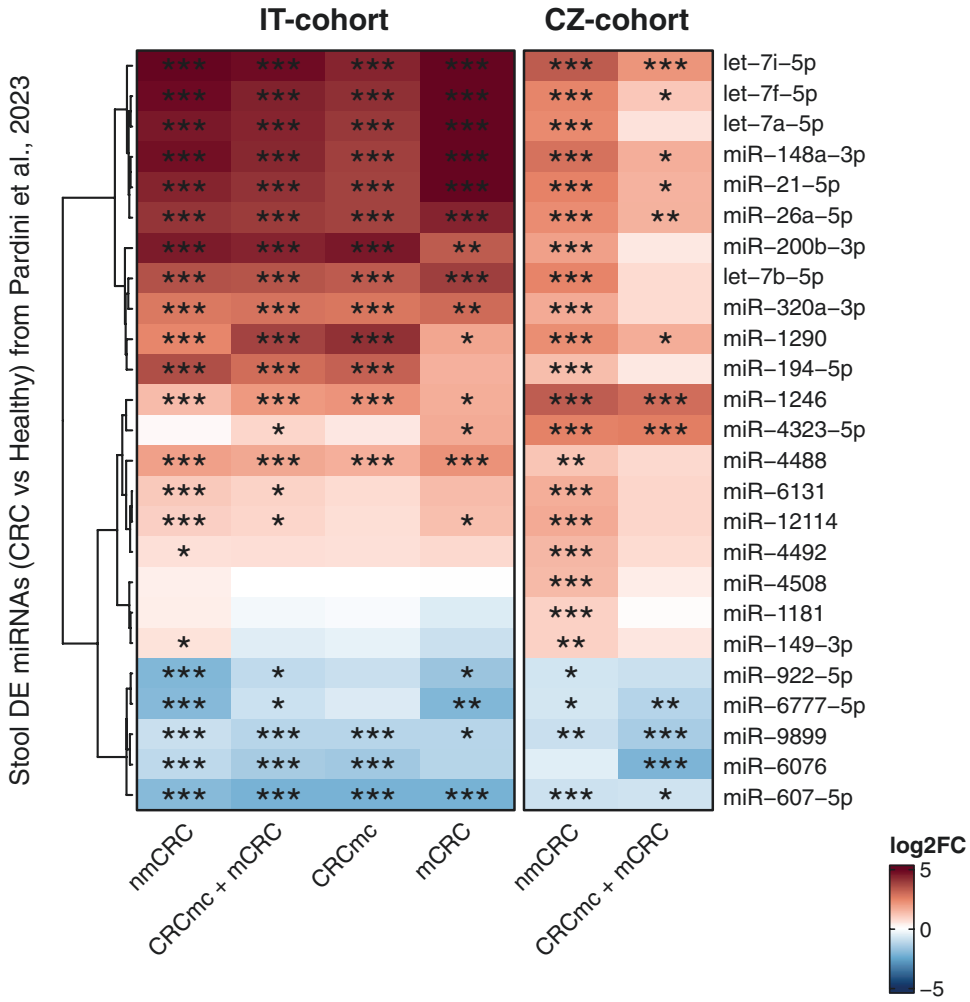

Figure 2. Heat map of the log2FC of the 25 fecal DE miRNAs identified in Pardini and colleagues [14] as measured in stool from patients with mucinous tumors (mCRC), with mucinous component < 50% (CRCmc), and non-mucinous (nmCRC). The plot reports the log2FC computed for the IT and CZ-cohorts considering the different CRC groups. *P*-value from DESeq2 analysis. *$P < .05$; **$P < .01$; ***$P < .001$.

Downloaded from https://academic.oup.com/mutage/advance-article/doi/10.1093/mutage/geae015/7689086 by Sapienza Università di Roma user on 30 June 2024

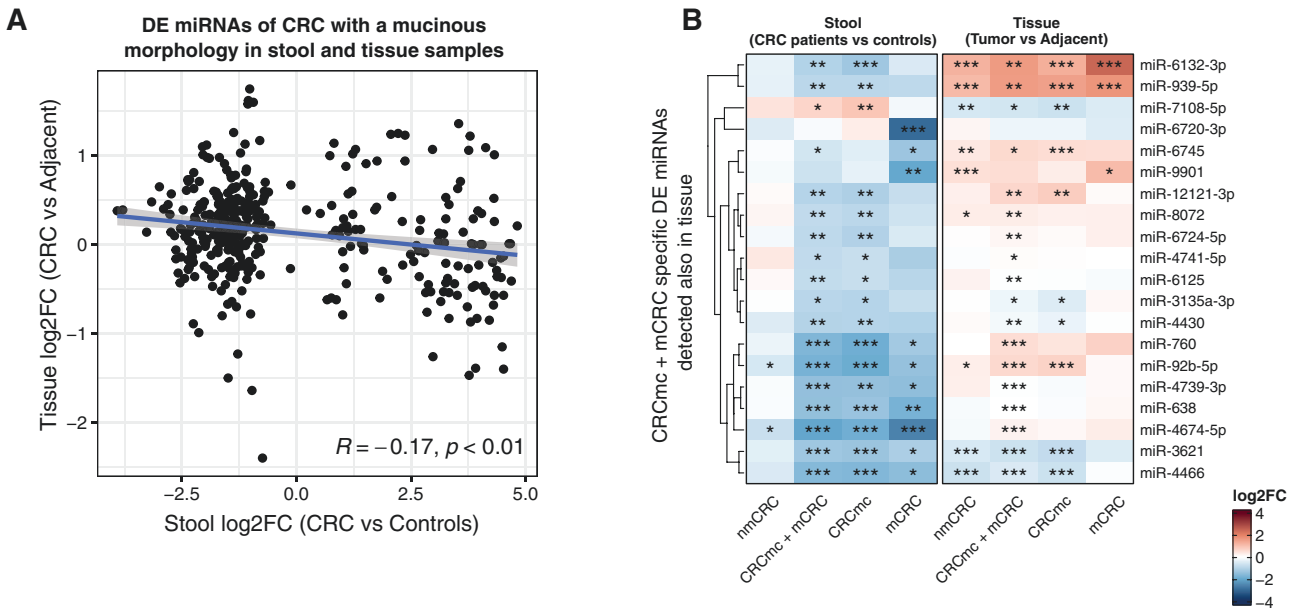

Figure 3. (A) Scatter plot of log2FC of stool DE miRNAs identified in samples with mucinous component < 50% (CRCmc) and mucinous CRC (mCRC) with respect to healthy controls. On the x-axis is reported the log2FC computed in the comparison of stool sample levels with respect to healthy subjects, while the y-axis reports the log2FC of expression computed between tumor and adjacent tissues. The results of the Spearman correlation analysis are reported. **(B)** Heat map of the log2FC of the 20 DE miRNAs identified as DE in stool and tissue of CRCmc and mCRC patient samples. *P*-value from DESeq2 analysis. **P* < .05; ***P* < .01; ****P* < .001.

analysis of both nmCRC and CRC with a mucinous morphology, 35 in nmCRC patients, while six (miR-101-3p, miR-181a-5p, miR-192-5p, miR-451a, miR-451b, miR-12121-3p, and miR-194-5p) only in tissue of CRCmc + mCRC patients (**Supplementary Table 1B**). Only miR-12121-3p was detected as specifically DE in both stool and tissue of patients with CRC with mucinous morphology.

Finally, among the 49 fecal DE miRNAs detected specifically in samples from CRC with a mucinous morphology, 20 were also detected in tissue samples from the same patients (**Fig. 3B** and **Supplementary Table 1B**). Among these miRNAs, 19 were characterized by levels significantly different in tumors with respect to adjacent colonic mucosa ($P < .05$), with 12 and 7 miRNAs, respectively, characterized by higher and lower levels in tumor samples. Two miRNAs, miR-3621 and miR-4466, were both associated with lower levels in the stool of CRC patients with respect to healthy controls and reduced levels in tumor samples with respect to adjacent mucosa (**Fig. 3B** and **Supplementary Table 1B**).

Discussion

In this study, we performed a comprehensive analysis of miRNA expression profiles in patients with CRC with or without a mucinous morphology, observing both distinct and common sets of miRNAs with significantly altered levels in fecal samples. Importantly, we explored whether mCRC and CRCmc presented or not a similar pattern of stool miRNA levels.

The analysis of the clinical data confirmed the known associations previously reported for CRC with a mucinous morphology in both categories (although mCRC were indeed few), including a higher prevalence of high-stage tumors characterized by *BRAF* mutations as well as MSI-high status [2]. A slightly higher localization of the mucinous lesions in the proximal colon was observed, albeit the difference was not statistically significant. mCRC were also characterized by a worst overall survival, as previously reported [18]. A possible reason for a shorter survival can be given by the fact that mucin glycoproteins form a barrier around tumor cells that further hides them from immune surveillance [19,20]. Moreover, mechanistic studies have shown that mucin glycoproteins have pro-tumorigenic potential per se. For example, MUC1 inhibits apoptosis by blocking the recruitment of caspase 8 [21]. Even though these observations that may explain the poor outcome of mucinous CRC patients, it is still very difficult to dissociate the barrier function of mucins from the intrinsic molecular tumorigenic function of these glycoproteins. Additional molecular experimental evidence is needed to unravel this.

A set of fecal miRNAs showed significantly decreased levels in both CRCmc and mCRC patients compared to healthy control subjects or nmCRC. Conversely, highly similar fecal miRNA profiles were observed between the two mucinous CRC subgroups, suggesting that a small mucinous component can already relate to a characteristic miRNA dysregulation. However, data on a higher number of mCRC patients are needed to confirm these observations. The list of fecal DE miRNAs identified in CRC with a mucinous morphology included miR-137-3p and miR-6125, whose downregulation was previously reported to be associated with CRC onset [22,23]. Interestingly, one of the targets of miR-6125, whose interaction is supported by the highest number of studies ($n = 3$), is *HSP90B1* that codes for the Glycoprotein 96 (GP96), a key player in the maintenance of the intestinal tissue homeostasis [24]. Despite these interesting aspects, more analyses are needed to clarify the regulatory activity of miR-6125 on *HSP90B1* expression and its candidate role in the mucinous CRC histotype definition. Interestingly, the glucose metabolism and response to oxygen levels were among the top significant terms enriched in the

Downloaded from https://academic.oup.com/mutage/advance-article/doi/10.1093/mutage/geae015/7689086 by Sapienza Università di Roma user on 30 June 2024

validated targets of the DE miRNAs identified in feces of CRCmc and mCRC patients. Intratumor metabolic heterogeneity was previously reported to be significantly higher in tumor with a mucinous component with respect to those from nmCRC [25]. A widespread downregulation of miRNA targeting metabolic processes could be a candidate factor involved in the exacerbation of this heterogeneity.

Fecal miRNA profiles in patients with CRC with a mucinous morphology were also explored with respect to the set of 25 fecal miRNAs that our group previously identified as specifically dysregulated in CRC patients with respect to healthy controls in a multicentric study [14]. The analysis confirmed altered miRNA levels in samples of all CRC subgroups, confirming these molecules as accurate biomarkers for the disease. Two miRNAs, miR-1181 and miR-149-3p, deserve attention. For these miRNAs, increased levels were originally reported in the whole cohort of CRC and in samples of nmCRC patients in comparison with healthy controls, while in CRCmc and mCRC they showed a (non-significant) different trend. In particular, miR-149-3p is a miRNA whose expression and release in extracellular vesicles was previously reported to be related to the gut microbiota composition [23,26]. Even if further investigations are needed, the observed differences in miR-149-3p expression could be linked to a differential composition of the microbial biofilm at the tumor surface, a factor that was previously proposed as a modulator of the onset of mucinous CRC histotype [27].

In tissue samples, DE miRNA analysis showed a similar trend of altered expression in CRCmc and mCRC with most of the miRNAs showing decreasing levels in tumor samples. Coherently, a decrease of miRNA levels in CRC with a mucinous morphology with respect to nmCRC has also been reported by Ruiz-Bañobre and colleagues [13]. Despite in our analysis none of these miRNAs showed a specific dysregulation in both mucinous subgroups, we confirmed the same expression trends as previously reported. Specifically, miR-1247-3p, miR-592, miR-1269a, and miR-552-3p were significantly decreased in CRC with a mucinous morphology ($P < .05$), while miR-31-5p was significantly more expressed in this histotype. miR-196b-3p was also significantly less expressed in CRCmc and mCRC, albeit the difference was not statistically significant in our dataset. The observed discrepancy between tissue and stool miRNA profiles in mCRC and CRCmc patients could be ascribed to different reasons. First, stool potentially collects extracellular miRNAs released by both the tumor cells and the whole intestinal tissue, making a direct comparison between tissue and stool profiles not trivial. In addition, we cannot exclude that the mucus layer may form a physical barrier perturbing the extent of extracellular miRNA release in the gut lumen, therefore explaining a higher dissimilarity between stool and tissue miRNA profiles in mucinous tumor than in other CRC. However, further investigations are needed to explore this hypothesis.

We are aware of certain limitations of this study. Although few differences were observed between CRCmc and mCRC, the number of mCRC subjects in our cohort was indeed low. This did not allow us to extensively evaluate the effect of possible confounding factors, like patient age and BMI, in the observed differences among CRC subtypes. Particularly, given the relevant role of obesity as risk factor of CRC development [28,29], it would be very interesting to explore the distribution of the mucinous CRC subtypes among obese patients. Therefore, a more extensive analysis of mCRC on a larger cohort is required to further support our findings together with a verification with qPCR or ddPCR of the most interesting signals. In our past work, we have performed qPCR experiments and confirmed specific miRNA signatures derived from sequencing [14,30]. Here, due to the limited size of study, cohort and the limiting availability of RNA, we could not perform this. In addition, although patient classification was performed by a central pathology review, this was performed considering only one tissue block for each patient, while the analysis of multiple blocks would be required to properly quantify the mucinous component. The development of a more objective quantification of the mucinous component and, therefore, the classification in CRCmc and mCRC is needed. Whilst the difference between these two subtypes is well understood, the current limitation is the 50% threshold that separates mucinous from non-mucinous cancers. In our opinion, the exact percentage of mucinous morphology should be reported in pathology reports for a better characterization of the tumor. Only with these detailed reports of mucinous morphology we could obtain the full spectrum of the clinical significance of the mucinous histotype. We believe that one solution to this limitation may be the quantification of molecular features (such as miRNAs) integrated with AI-based tools that automatically quantify the percentage of mucinous morphology across all tumor slides of a patient. Finally, since the identification of the cellular origin of stool miRNAs is not trivial, it will be valuable to explore the specific tissue localization of the DE miRNAs identified in both analyzed sample types. This analysis would provide further details on the cellular expression or the extracellular release colocalized with the mucinous component or with a specific cellular population of the tumor microenvironment.

Despite the above limitations, our study represents the first multi-specimen analysis of miRNA profiles in samples of CRC patients stratified quantitatively by mucinous morphology. Globally, we did not observe remarkable differences in fecal/tissue miRNA levels between CRCmc and mCRC, with few exceptions, with mostly significantly coherent expression changes with respect to healthy controls/adjacent mucosa. In the ongoing debate on the definition of mucinous CRC, based solely on the threshold of 50% of mucinous component and strongly related to specific molecular and clinical features, our results demonstrated that the mode of definition of this subtype may be not sufficient and we will need more biomarkers and features to refine this classification.

In future investigations, the obtained results will be integrated with information from additional omics, including the total RNA transcriptome, the gut and intratumor microbial content, and mutational status.

Supplementary data

Supplementary data is available at *Mutagenesis* Online.

Acknowledgements

The authors would like to thank all the subjects who contributed to the research with their biological samples and the data necessary for our studies. The authors are also grateful to all the personnel in the hospitals and in the labs who have participated in the collection of the samples and the wet-lab or computational analyses. We would also like to thank Giuseppe Gaeta and Ines Koch for their technical assistance.

Downloaded from https://academic.oup.com/mutage/advance-article/doi/10.1093/mutage/geae015/7689086 by Sapienza Università di Roma user on 30 June 2024

Conflict of interest

All authors report no competing interests except for TB that reports the following statements: speaker for Roche, Astellas, Janssen, Bristol Myers Squibb, and Merck; advisory board member for Bayer, Bristol Myers Squibb, Ipsen, Merck, Servier, Eli Lilly, Pfizer, and Accord; institutional support from Bristol Myers Squibb, Astra Zeneca, Merck, Bayer, Exelixis, Eisai, Eli Lilly, Roche, and MSD. This publication reflects only the author's view and the European Commission is not responsible for any use that may be made of the information it contains.

Funding

This work was supported by the Italian Institute for Genomic Medicine (IIGM) and Compagnia di San Paolo Torino, Italy (to AN, BP, and ST). This project has received funding from the European Union`s Horizon 2020 research and innovation program under grant agreement No 825410 (ONCOBIOME project to AN, BP, and ST). The research leading to these results has received funding from AIRC under IG 2020—ID. 24882—P.I. Naccarati Alessio Gordon (to AN). The work of Dr Dragomir is supported by the Berlin Institute of Health (CS Program) and by DKTK Berlin (Young Investigator Grant 2022).

Data availability

Raw data are available upon request to the corresponding author.

References

1. Fleming M, Ravula S, Tatishchev SF, *et al*. Colorectal carcinoma: Pathologic aspects. *J Gastrointest Oncol* 2012;**3**:153–73.
2. Huang A, Yang Y, Shi JY, *et al*. Mucinous adenocarcinoma: A unique clinicopathological subtype in colorectal cancer. *World J Gastrointest Surg* 2021;**13**:1567–83.
3. Nagtegaal ID, Odze RD, Klimstra D, *et al*. The 2019 WHO classification of tumours of the digestive system. *Histopathology* 2020;**76**:182–8.
4. Hugen N, Brown G, Glynne-Jones R, *et al*. Advances in the care of patients with mucinous colorectal cancer. *Nat Rev Clin Oncol* 2016;**13**:361–9.
5. Onodera M, Nishigami T, Torii I, *et al*. Comparison between colorectal low- and high-grade mucinous adenocarcinoma with MUC1 and MUC5AC. *World J Gastrointest Oncol* 2009;**1**:69–73.
6. Li WQ, Kawakami K, Ruszkiewicz A, *et al*. BRAF mutations are associated with distinctive clinical, pathological and molecular features of colorectal cancer independently of microsatellite instability status. *Mol Cancer* 2006;**5**:2.
7. Wang MJ, Ping J, Li Y, *et al*. Prognostic significance and molecular features of colorectal mucinous adenocarcinomas: A strobe-compliant study. *Medicine (Baltim)* 2015;**94**:e2350.
8. Verhulst J, Ferdinande L, Demetter P, *et al*. Mucinous subtype as prognostic factor in colorectal cancer: a systematic review and meta-analysis. *J Clin Pathol* 2012;**65**:381–8.
9. McCawley N, Clancy C, O'Neill BD, *et al*. Mucinous rectal adenocarcinoma is associated with a poor response to neoadjuvant chemoradiotherapy: A systematic review and meta-analysis. *Dis Colon Rectum* 2016;**59**:1200–8.
10. Dragomir MP, Knutsen E, Calin GA. Classical and noncanonical functions of miRNAs in cancers. *Trends Genet* 2022;**38**:379–94.
11. Cantini L, Isella C, Petti C, *et al*. MicroRNA-mRNA interactions underlying colorectal cancer molecular subtypes. *Nat Commun* 2015;**6**:8878.
12. Slattery ML, Herrick JS, Mullany LE, *et al*. Colorectal tumor molecular phenotype and miRNA: expression profiles and prognosis. *Mod Pathol* 2016;**29**:915–27.
13. Ruiz-Banobre J, Roy R, Alustiza Fernandez M, *et al*. Clinical significance of a microRNA signature for the identification and predicting prognosis in colorectal cancers with mucinous differentiation. *Carcinogenesis* 2020;**41**:1498–506.
14. Pardini B, Ferrero G, Tarallo S, *et al*. A fecal microRNA signature by small RNA sequencing accurately distinguishes colorectal cancers: Results from a multicenter study. *Gastroenterology* 2023;**165**:582–99.e8.
15. Gagliardi A, Francescato G, Ferrero G, *et al*. The 8q24 region hosts miRNAs altered in biospecimens of colorectal and bladder cancer patients. *Cancer Med* 2023;**12**:5859–73.
16. Tarallo S, Ferrero G, Gallo G, *et al*. Altered fecal small RNA profiles in colorectal cancer reflect gut microbiome composition in stool samples. *mSystems* 2019;**4**:e00289–19.
17. Tarallo S, Ferrero G, De Filippis F, *et al*. Stool microRNA profiles reflect different dietary and gut microbiome patterns in healthy individuals. *Gut* 2022;**71**:1302–14.
18. Zhang Y, Chen Y, Huang J, *et al*. Mucinous histology is associated with poor prognosis in locally advanced colorectal adenocarcinoma treated with postoperative first-line adjuvant chemotherapy: A systematic review and meta-analysis. *Eur J Surg Oncol* 2022;**48**:2075–81.
19. O'Connell E, Reynolds IS, McNamara DA, *et al*. Resistance to cell death in mucinous colorectal cancer-a review. *Cancers (Basel)* 2021;**13**:1389.
20. Kufe DW. Mucins in cancer: function, prognosis and therapy. *Nat Rev Cancer* 2009;**9**:874–85.
21. Agata N, Ahmad R, Kawano T, *et al*. MUC1 oncoprotein blocks death receptor-mediated apoptosis by inhibiting recruitment of caspase-8. *Cancer Res* 2008;**68**:6136–44.
22. Balaguer F, Link A, Lozano JJ, *et al*. Epigenetic silencing of miR-137 is an early event in colorectal carcinogenesis. *Cancer Res* 2010;**70**:6609–18.
23. Feng Q, Li Y, Zhang H, *et al*. Deficiency of miRNA-149-3p shaped gut microbiota and enhanced dextran sulfate sodium-induced colitis. *Mol Ther Nucleic Acids* 2022;**30**:208–25.
24. Hafliger J, Schwarzfischer M, Atrott K, *et al*. Glycoprotein (GP)96 is essential for maintaining intestinal epithelial architecture by supporting its self-renewal capacity. *Cell Mol Gastroenterol Hepatol* 2023;**15**:717–39.
25. Zhang L, Liu Y, Ding Y, *et al*. Predictive value of intratumoral-metabolic heterogeneity derived from (18)F-FDG PET/CT in distinguishing microsatellite instability status of colorectal carcinoma. *Front Oncol* 2023;**13**:1065744.
26. Cao Y, Wang Z, Yan Y, *et al*. Enterotoxigenic bacteroidesfragilis promotes intestinal inflammation and malignancy by inhibiting exosome-packaged miR-149-3p. *Gastroenterology* 2021;**161**:1552–66.e12.
27. Li S, Peppelenbosch MP, Smits R. Bacterial biofilms as a potential contributor to mucinous colorectal cancer formation. *Biochim Biophys Acta Rev Cancer* 2019;**1872**:74–9.
28. Ye P, Xi Y, Huang Z, *et al*. Linking obesity with colorectal cancer: epidemiology and mechanistic insights. *Cancers (Basel)* 2020;**12**:1408.
29. Seo JY, Jin EH, Chung GE, *et al*. The risk of colorectal cancer according to obesity status at four-year intervals: a nationwide population-based cohort study. *Sci Rep* 2023;**13**:8928.
30. Pardini B, Cordero F, Naccarati A, *et al*. microRNA profiles in urine by next-generation sequencing can stratify bladder cancer subtypes. *Oncotarget* 2018;**9**:20658–69.

Downloaded from https://academic.oup.com/mutage/advance-article/doi/10.1093/mutage/geae015/7689086 by Sapienza Università di Roma user on 30 June 2024